J Solid State Electrochem (2006) 10: 581–588
DOI 10.1007/s10008-006-0130-2

ORIGINAL PAPER

Jaap F. Vente · Steven McIntosh · Wim G. Haije · Henny J. M. Bouwmeester

Properties and performance of $Ba_xSr_{1-x}Co_{0.8}Fe_{0.2}O_{3-\delta}$ materials for oxygen transport membranes

Received: 23 December 2005 / Accepted: 7 January 2006 / Published online: 3 May 2006

Abstract The present paper discusses the oxygen transport properties, oxygen stoichiometry, phase stability, and chemical and mechanical stability of the perovskites $Ba_{0.5}Sr_{0.5}Co_{0.8}Fe_{0.2}O_{3-\delta}$ (BSCF) and $SrCo_{0.8}Fe_{0.2}O_{3-\delta}$ (SCF) for air separation applications. The low oxygen conductive brownmillerite phase in SCF is characterized using in-situ neutron diffraction, thermographic analysis and temperature programmed desorption but this phase is not present for BSCF under the conditions studied. Although both materials show oxygen fluxes well above 10 ml/cm^2·min at T=1,273 K and pO_2=1 bar for self-supporting, 200 μm-thick membranes, BSCF is preferred as a membrane material due to its phase stability. However, BSCF's long-term stable performance remains to be confirmed. The deviation from ideal oxygen stoichiometry for both materials is high: δ>0.6. The thermal expansion coefficients of BSCF and SCF are 24×10^{-6} and 30×10^{-6} K^{-1}, respectively, as determined from neutron diffraction data. The phenomenon of kinetic demixing has been observed at $pO_2<10^{-5}$ bar, resulting in roughening of the surface and enrichment with alkaline earth metals. Stress–strain curves were determined and indicated creep behavior that induces undesired ductility at T=1,073 K for SCF. Remedies for mechanical and chemical instabilities are discussed.

J. F. Vente (✉) · W. G. Haije
Energy research Centre of the Netherlands (ECN),
P.O. Box 1, 1755 ZG Petten, The Netherlands
e-mail: vente@ecn.nl
Tel.: +31-224-564916
Fax: +31-224-568615

S. McIntosh · H. J. M. Bouwmeester
Inorganic Materials Science,
Faculty of Science and Technology and
MESA+ Institute for Nanotechnology, University of Twente,
P.O. Box 217, 7500 AE Enschede, The Netherlands

Present address:
S. McIntosh
Department of Chemical Engineering, University of Virginia,
Charlottesville, VA 22904-4741, USA

Keywords $Ba_xSr_{1-x}Co_{0.8}Fe_{0.2}O_{3-\delta}$ · Oxygen transport membranes · Phase relation · Mechanical strength · Chemical stability

Introduction

Mixed ionic–electronic conducting oxides with the perovskite structure are of interest as ceramic membranes for the energy-efficient separation of oxygen from air, for the production of syngas from hydrocarbons, and as electrode materials for solid oxide fuel cells. The primary research objectives related to these materials are flux optimization; increased chemical stability, especially under reducing conditions; mechanical stability; and insight into the transport mechanism, i.e., bulk and surface phenomena. Two of the most promising materials for air separation are $SrCo_{0.8}Fe_{0.2}O_{3-\delta}$ (SCF) and $Ba_{0.5}Sr_{0.5}Co_{0.8}Fe_{0.2}O_{3-\delta}$ (BSCF). SCF was first reported by Teraoka et al. in 1985 to have the highest oxygen permeability in the system $Sr_{1-x}La_xCo_{1-y}Fe_yO_{3-\delta}$ [1]. Later experiments were designed to elucidate whether the bulk diffusivity or the surface reaction process was the rate-limiting step for oxygen permeation. Based on SCF membranes with thicknesses ranging between 1 and 5 mm, Qiu et al. [2] concluded that the surface effects were rate determining. This was substantiated by the observation that the fluxes could be enhanced through the application of thin, porous, so-called activation layers of the same material on the membrane surface [3]. Neutron diffraction measurements on membranes operating with air on the feed side and a mixture of CO and CO_2 on the permeate side demonstrated that the lattice constant is close to that in air across the membrane, suggesting an oxygen stoichiometry profile that is shallow across the membrane and steep at the low pO_2 surface [4]. This observation is consistent with the rate-limiting surface reaction located at the permeate side.

The high-temperature mechanical properties [5], phase relation dependence on the pO_2 and temperature [4, 6], and

oxygen nonstoichiometry [7–9] have been the subject of other recent research activities. In addition, the dual-phase membrane SCF–$SrSnO_3$ was developed [10] with the aim to increase the thermochemical compatibility by reducing the thermal expansion coefficient and inhibiting the growth of the grains. An alternative approach is to study B-cation substitutions, including Ag^{+} [11], Ca^{2+}, Ti^{4+}, and Zr^{4+} [12], to enhance phase stability and improve oxygen permeability. The rationale for the development of BSCF membranes was the suggested chemical stability of this A-cation substituted compound in 2000 [13]. It should be borne in mind that these cobalt-rich materials are suitable candidates for membranes for air separation. When highly reducing conditions are present, as in the partial oxidation of hydrocarbons, one should replace Co with less-reducible cations, as in $La_xSr_{1-x}Fe_yGa_{1-y}O_{3-\delta}$ [14, 15], or switch over to oxygen excess compounds with the K_2NiF_4 structure, such as $La_2Ni_{2-x}M_xO_{4+\delta}$ [16].

In this short overview, we will bring together the information currently available on the compounds in the system $Ba_xSr_{1-x}Co_{0.8}Fe_{0.2}O_{3-\delta}$, with an emphasis on the x=0.0 and 0.5 members. Further, we will provide some previously unpublished results.

Oxygen permeability

The applicability of perovskite-based membranes for air separation largely depends on the oxygen flux, as this determines the membrane surface area required and, therefore, the initial capital cost. Bredesen and Sogge [17] estimated a minimum value of 10 ml/cm^2·min for economic viability. Figure 1 shows the oxygen fluxes for flat, self-supporting functional membranes of SCF, BSCF, and $La_{0.2}Sr_{0.8}Co_{0.8}Fe_{0.2}O_{3-\delta}$ (LSCF). The membranes were 200 μm thick with effective surface areas of 18 cm^2. A mixture of oxygen and nitrogen was fed to the membrane with a total flow of 500 ml/min STP, while helium ($pO_2 \approx 10^{-5}$ bar) was used as a sweep gas at 600 ml/min STP. The partial oxygen pressure at the outlet of the permeate side was dependent on the oxygen flux and ranged from 0.02 to 0.28 bar. A more detailed description of the measurement set up can be found in reference [18]. At 973 K (Fig. 1a), the flux increases on going from LSCF to SCF, and finally to BSCF, independent of the partial feed pressure of oxygen. As may be anticipated, the fluxes increase when the temperature is increased to 1,273 K (Fig. 1b). However, the difference in oxygen flux between SCF and BSCF decreases significantly. The oxygen flux through both membranes is higher than the 10 ml/cm^2·min target even with an oxygen partial-feed pressure three times lower than that under industrial conditions, where a total air pressure of 16 bar will be used [19].

The large difference between SCF and BSCF oxygen fluxes at low temperature has been ascribed to the presence of the vacancy ordered brownmillerite phase in SCF (δ=0.5) [20, 21]. This brownmillerite phase has been reported to have low oxygen permeability [22] with the observed reduced oxygen fluxes attributed to the coexistence of the brownmillerite and perovskite phases. The transformation of the brownmillerite form of LSCF into the cubic perovskite phase occurs at a temperature similar to that of SCF [8]. The reported perovskite phase with this composition has a smaller concentration of oxygen vacancies ($0.15<\delta<0.35$ for T=823 K and $10^{-5}<pO_2/\text{bar}<1$) than SCF ($\delta>0.6$) and BSCF ($\delta>0.65$) (see also Fig. 2). The differences in flux at 1,273 K can thus be ascribed to differences in oxygen nonstoichiometry. That is, decreased oxygen content in the cubic perovskite leads to increased flux. This will be discussed further in the next section.

The oxygen permeability of SCF was reported to be dependent on the grain size [23]. A 30% decrease in oxygen flux was observed when the grain size was increased from 4 to 14 μm using disc-shaped samples with a thickness of ~2 mm. Two explanations have been proposed: that the grain boundaries in the sample provide a faster transport path for the oxygen diffusion or that the surface exchange rate is enhanced by the grain boundaries. Contrary to this, Wang et al. [24] observe an increase of oxygen flux with increasing grain size for BSCF. This apparent disagreement can only be resolved by carefully preparing samples with different thicknesses and a controlled grain size of one composition. A more general discussion on the influence of the ceramic microstructure and the oxygen permeability has been published by Kharton and Marques [25].

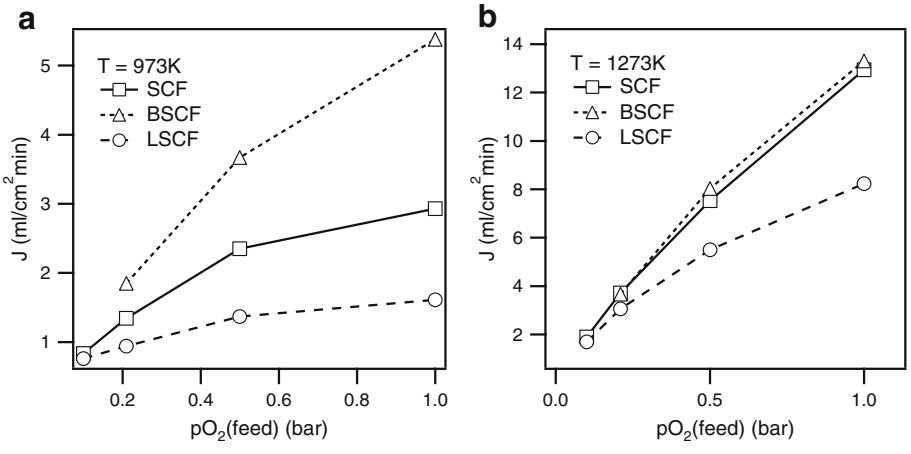

Fig. 1 The oxygen fluxes for SCF, BSCF, and LSCF as a function of the pO_2 at the feed side at 973 (**a**) and 1,273 K (**b**); pO_2 at the exit of the permeate ranges from 0.02 to 0.28 bar

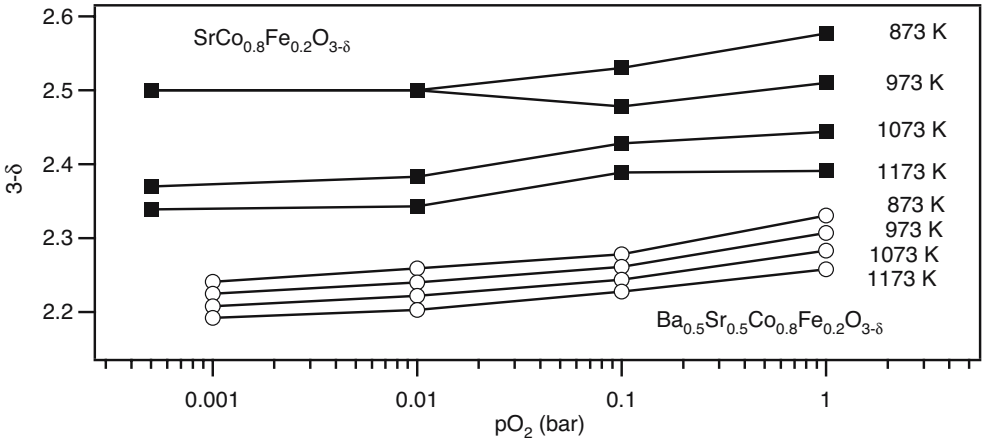

Fig. 2 Oxygen stoichiometry (3-δ) as a function of pO_2 and temperature for SCF and BSCF determined by in-situ neutron diffraction

Under certain conditions, SCF and BSCF can react with H_2O and CO_2 to form hydrates and carbonates. This is undesirable as the compounds formed have much lower oxygen permeability than the original materials. Yi et al. [26] report a reduced oxygen flux for SCF at 1,085 K only when the feed gas contained both CO_2 and H_2O. The flux was almost unaffected at 1,175 K or when only one of these components was present at 1,085 K. Such an effect has also been observed for $BaCo_{0.4}Fe_{0.4}Zr_{0.2}O_{3-\delta}$ [27] where the oxygen flux at temperatures <1,125 K was found to reduce strongly in the presence of CO_2, especially on the permeate side.

Oxygen stoichiometry and phase stability

At high temperatures (>1,064 K), both SCF and BSCF adopt the cubic perovskite structure as depicted in Fig. 3a. In this structure, all Co/Fe cations are in regular octahedral coordination and all oxygen sites are chemically equiva-

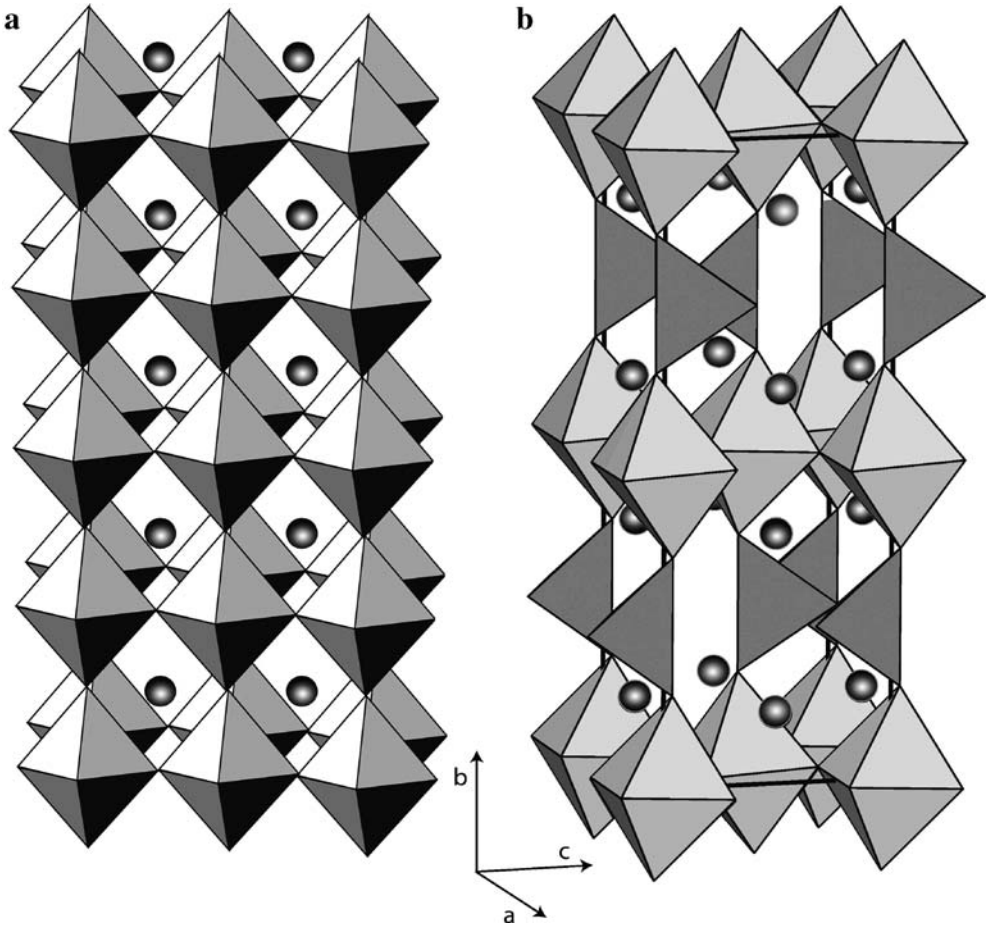

Fig. 3 Polyhedral representations of the cubic perovskite (**a**) and brownmillerite (**b**) phases. The *circles* represent the positions of A-site cations

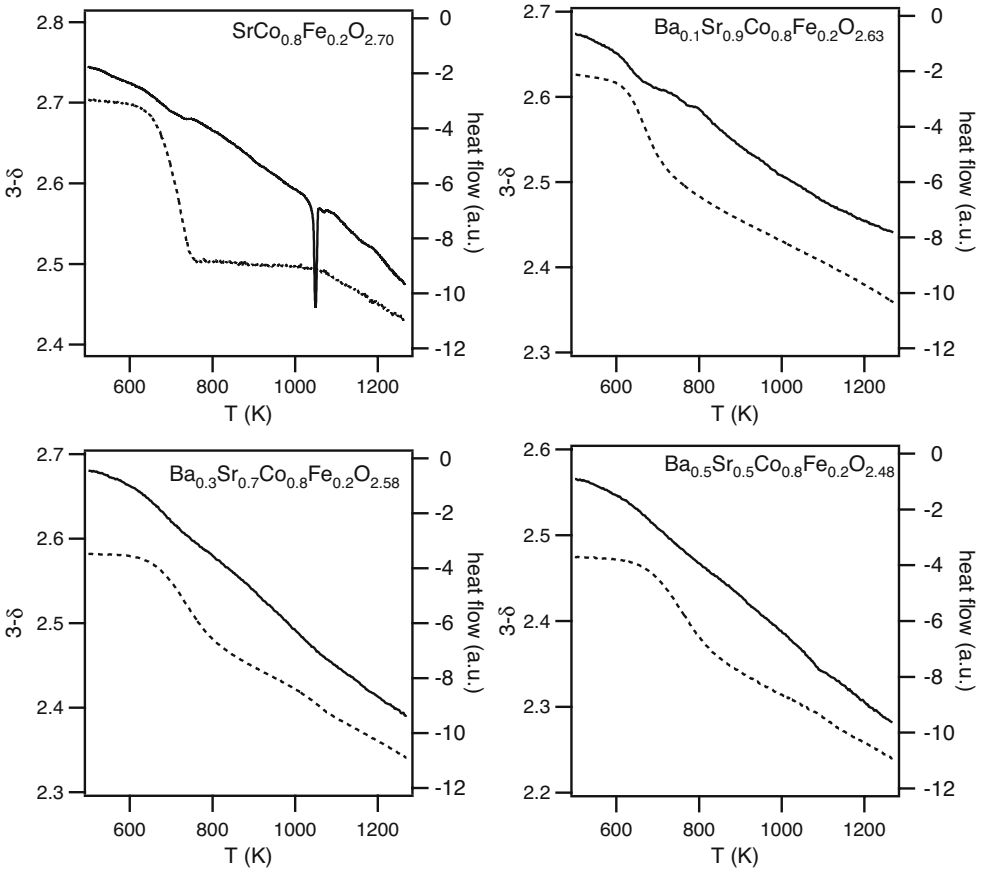

Fig. 4 Oxygen stoichiometry (3-δ) (*dashed line*) and the endothermic heat flow (*full line*) for $Ba_xSr_{1-x}Co_{0.8}Fe_{0.2}O_{3-\delta}$ as determined on heating in nitrogen at 10 K/min using TGA–differential thermal analysis. The powdered samples were previously cooled in air at 0.5 K/min

lent. At lower temperatures and with reduced oxygen partial pressure, oxygen vacancy ordering occurs in SCF, resulting in a phase transition from cubic perovskite to orthorhombic brownmillerite (Fig. 3b). In the brownmillerite structure, ideal composition $A_2B_2O_5$, the oxygen vacancies are ordered along rows in the [1 0 1] direction of the brownmillerite cell. This results in alternating layers of BO_6 octahedra and BO_4 tetrahedra perpendicular to the b-axis. Both polyhedra are distorted, especially the tetrahedra, and splitting of the B-cation sites can occur (McIntosh et al. submitted for publication). The ordered vacancies in the brownmillerite phase are reported to be immobile, leading to decreased oxygen anion permeability [20]. Small deviations from the ideal oxygen stoichiometry, $A_2B_2O_5$, may introduce mobile vacancies into the octahedral layer. However, recent high-temperature neutron diffraction experiments have revealed that the concentration of these vacancies does not exceed 0.02 per formula unit [6]. This is an order of magnitude lower than the vacancy concentration in the perovskite [6, 28]. The brownmillerite phase is not stabilized for BSCF, and the compound maintains the cubic perovskite structure over the same pO_2 and temperature range [28].

In Fig. 2, we compare the oxygen stoichiometry (3-δ) of SCF [6] with BSCF [28] at different temperatures and partial oxygen pressures as determined by neutron diffraction studies. Under all measurement conditions, the oxygen stoichiometry of SCF is higher than that of BSCF. The pO_2 range where brownmillerite can be stabilized as a single phase between 873 and 973 K is shown by the constant oxygen stoichiometry, 3-δ, of 2.5. Figure 2 also clearly shows that in the single-phase perovskite region, the oxygen stoichiometry of SCF is more dependent on temperature than that of BSCF. This is likely one of the origins of the smaller total expansion coefficient of BSCF compared to SCF, as will be discussed below.

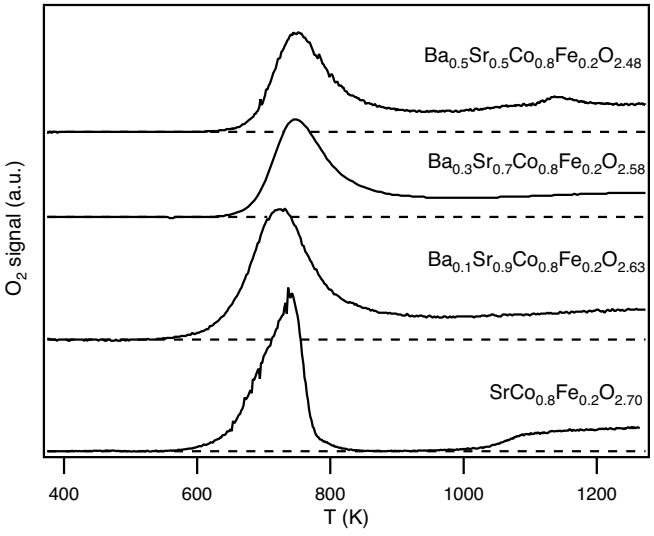

Fig. 5 The relative oxygen release rate for $Ba_xSr_{1-x}Co_{0.8}Fe_{0.2}O_{3-\delta}$ upon heating in nitrogen at 10 K/min as determined by TPD. The powdered samples were previously cooled in air at 0.5 K/min

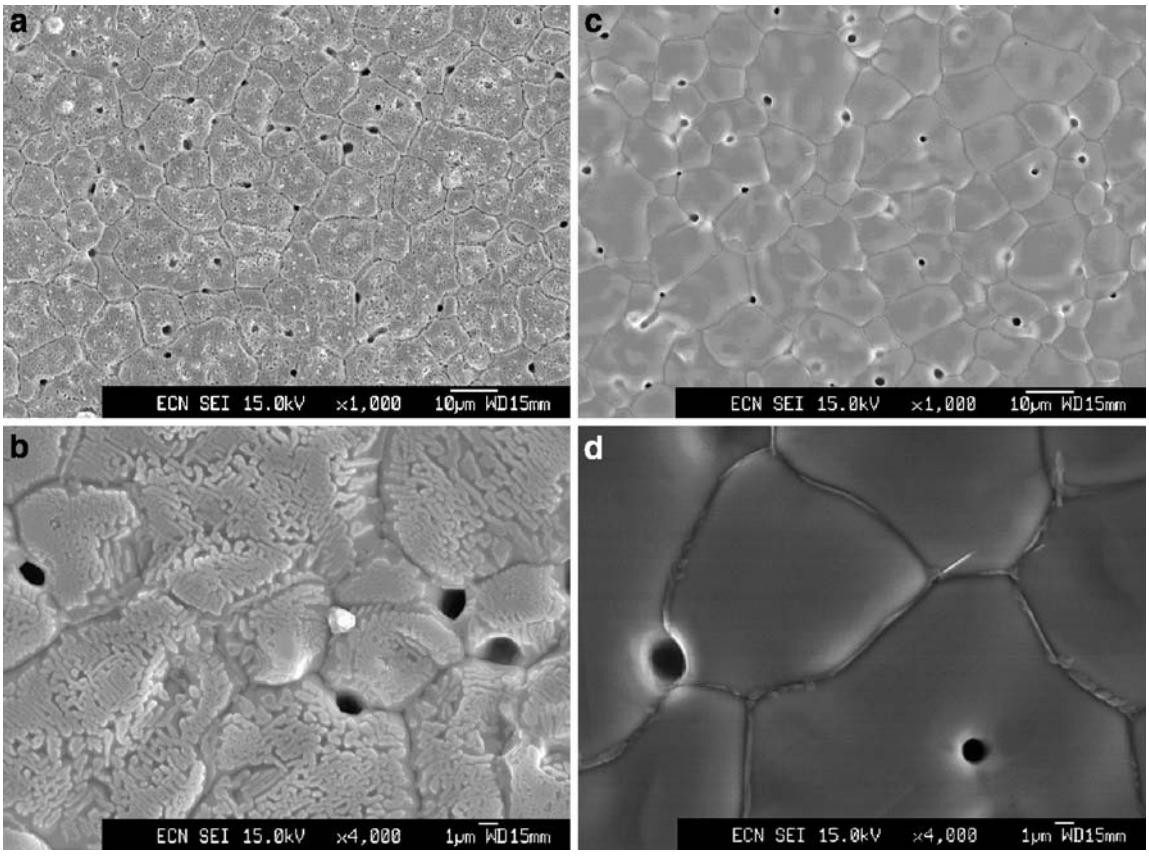

Fig. 6 Post test SEM micrographs of a BSCF membrane after being measured between $973 \leq T/K \leq 1{,}273$ and $0.1 \leq pO_2/bar \leq 1$ for 3 weeks with graphs (**a**) and (**b**) taken at a position close to and graphs (**c**) and (**d**) at a position far away from the helium inlet

The formation of the brownmillerite phase can also be recognized in thermographic analysis (TGA), differential scanning calorimetry, and temperature programmed desorption (TPD) measurements. In Fig. 4, we show the oxygen stoichiometry of four samples in the system $Ba_xSr_{1-x}Co_{0.8}Fe_{0.2}O_{3-\delta}$ as a function of temperature during heating in grade 5.0 nitrogen. The samples were previously cooled in air at 0.5 K/min from 1,373 K. The TPD of oxygen measured under similar conditions is presented in Fig. 5. Our TPD graphs are very distinct from those reported earlier [13]. This can be attributed to differences in the thermochemical history of the sample, in sample and particle size, and in gas flow rates used. Due to the slow cooling in air and the transfer of the sample to a low-pO_2 environment at room temperature, there is an excess of oxygen in the structure when compared to that expected for equilibrium with a gas pO_2 of 6×10^{-6} bar. We may then expect oxygen release upon heating. Both Figs. 4 and 5 show that no release of any oxygen occurs up to ~575 K as the nonequilibrium, or "excess," oxygen is kinetically trapped in the structure. Under the current conditions, the kinetics become sufficiently fast to allow for the equilibration of the oxygen stoichiometry at ~575 K, where the TPD signal shows a single peak, and the TGA shows a sudden decrease in stoichiometry. Above 800 K, the brownmillerite phase in SCF can be recognized by a zero-oxygen release rate and an oxygen stoichiometry of 2.5. Only at temperatures above ~1,050 K does oxygen release resume. At the same temperature, an endothermic peak is observed in the differential thermal analysis signal. These observations are consistent with the order–disorder transition from the brownmillerite to the perovskite phase.

The oxygen release, as determined in the TPD measurements (Fig. 5), of the samples $Ba_xSr_{1-x}Co_{0.8}Fe_{0.2}O_{3-\delta}$ with $x>0$ did not reduce to 0 after the peak centered at ~700 K, and the oxygen content in these samples decreased continuously, as can be seen from the TGA signal (Fig. 4). For BSCF, this is consistent with the observation from Fig. 2 that BSCF adopts the cubic perovskite structure under all conditions studied. The same can therefore be inferred for the compounds $Ba_xSr_{1-x}Co_{0.8}Fe_{0.2}O_{3-\delta}$ with x=0.1 and 0.3.

One of the greatest challenges to overcome for the application of the current materials is their limited stability under a gradient of oxygen chemical potential and high oxygen flux. As a consequence of differences in the self-diffusion coefficients for the elements present under the influence of a gradient of the chemical potential, significant enrichment of the alkaline earth metals on the permeate side may occur. This so-called kinetic demixing has been observed for $La_{0.6}Sr_{0.4}Co_{0.2}Fe_{0.8}O_{3-\delta}$ [18] and $La_{0.3}Sr_{0.7}CoO_{3-\delta}$ [29]. In the case of BSCF, we observed a similar enrichment near the helium inlet where the pO_2 is relatively low in agreement with Van Veen et al. [30]. The surface in this region (Fig. 6a,b) becomes very rough and the grain

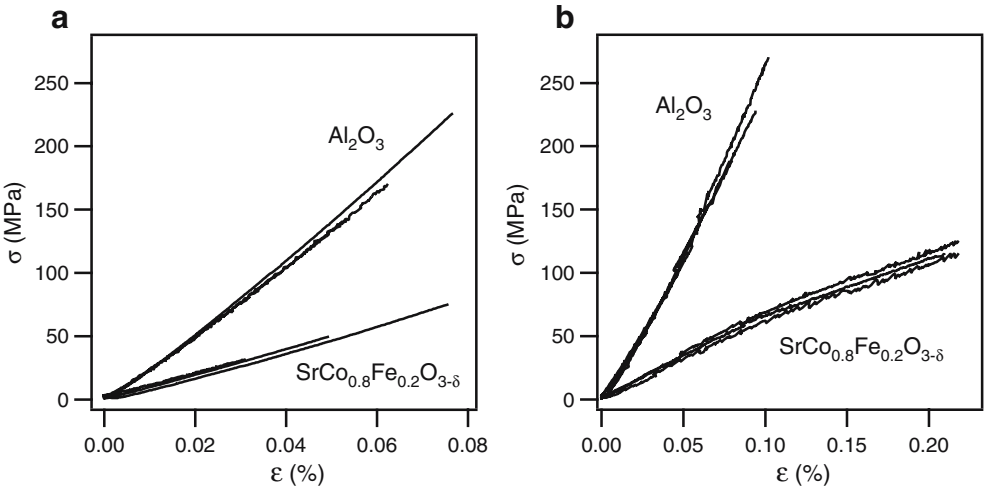

Fig. 7 Ring-on-ring stress–strain diagrams for Al_2O_3 and SCF at room temperature (**a**) and at 1,073 K (**b**)

boundaries appear to be etched away after 3 weeks of testing between 973 and 1,273 K. This surface reconstruction has also been observed on a surface exposed to methane by Wang et al. [31]. The SEM micrographs shown in Fig. 6c,d are taken far away from the helium inlet, where the pO_2 is relatively high. The surface here is smooth and very similar to that on the feed side, high pO_2, after the permeation experiment and to the surface before the test. No significant deviation from the original composition was observed. The posttest grain size appeared to be independent of the location on the membrane and ranged from 10 to 20 μm.

The discussion above has been limited to partial oxygen pressures higher than $\sim 10^{-5}$ bar. At lower pO_2 the phases present are expected to decompose. Li et al. [4] examined the stability of SCF membranes at 1,173 K using neutron diffraction techniques. They found that below a pO_2 of $\sim 10^{-14}$ bar, the cubic perovskite phase decomposes into a three-phase mixture consisting of two Ruddlesden–Popper phases, $Sr_{n+1}(Fe,Co)_nO_{(3n+1-\delta)}$ with n=2 and 3 and CoO with the rocksalt structure.

Mechanical issues

The expansion behavior is an import issue when it comes to the application of $Ba_xSr_{1-x}Co_{0.8}Fe_{0.2}O_{3-\delta}$ as a membrane material and it is closely related to composition and phase stability. In an industrial application, the ceramic material must be connected to the material of the membrane module, most likely steel. The thermal and chemical expansion coefficients influence the compatibility of these materials and place stringent demands on the seals. The compounds $Ba_xSr_{1-x}Co_{0.8}Fe_{0.2}O_{3-\delta}$ expand on heating and on partial reduction. As a result, three types of expansion can be distinguished. The total, chemical, and thermal expansion coefficients are determined at constant pO_2, constant T, and constant oxygen stoichiometry, respectively [32]. The averaged total expansion coefficient in the temperature range 300≤T/K<1,300 in air of BSCF, as determined by high-temperature X-ray diffraction experiments, is $\sim 12\times10^{-6}$ K^{-1}, being significantly smaller than that of SCF, 18×10^{-6} K^{-1}, under the same conditions [24]. These values compare to those determined by in-situ neutron diffraction measured in the smaller temperature range of 875≤T/K≤1,175 of $\sim 24\times10^{-6}$ and $\sim 30\times10^{-6}$ K^{-1} [6]. The origin of the difference between the values determined by these two methods can be found in the far-from-linear behavior of the temperature dependence of the total expansion coefficient, as can be concluded from dilatometry data [21]. Alternatively, a different choice of the reference state results in somewhat different values. For comparison, the values for plain carbon steel and stainless steel 304 are 11.7×10^{-6} and 17.3×10^{-6} K^{-1}, respectively [33]. At low partial pressures, pO_2<0.1 bar, the difference between the two perovskites is even larger. The total thermal expansion of SCF is influenced by the transition from the brownmillerite phase to the cubic perovskite phase. At this transition, the volume per formula unit reduces by more than 1% [6], which is reflected by a negative total thermal expansion coefficient over a limited temperature range in dilatometry [21]. The lower total expansion coefficient of BSCF may be related to a smaller dependence of the oxygen nonstoichiometry on the temperature. The possible formation of the brownmillerite phase has important implications for the thermal cycling of SCF membranes under pO_2 gradients. Very low partial oxygen pressures, however, are not foreseen in SCF applications, and therefore, chemical stability will be the more important issue. Nevertheless, BSCF is preferred as a membrane material in view of operational reliability in membrane applications.

A further important issue is the mechanical integrity. Under industrial conditions a pressure difference of about 16 bar is applied over the membrane at around 1,100 K [19]. Full mechanical integrity is prerequisite. Ring-on-ring tests (equibiaxial bending test) have been performed on SCF discs in comparison with alumina reference material at room temperature and 1,073 K. Discs of both materials were about 40 mm in diameter and 0.6 mm thick

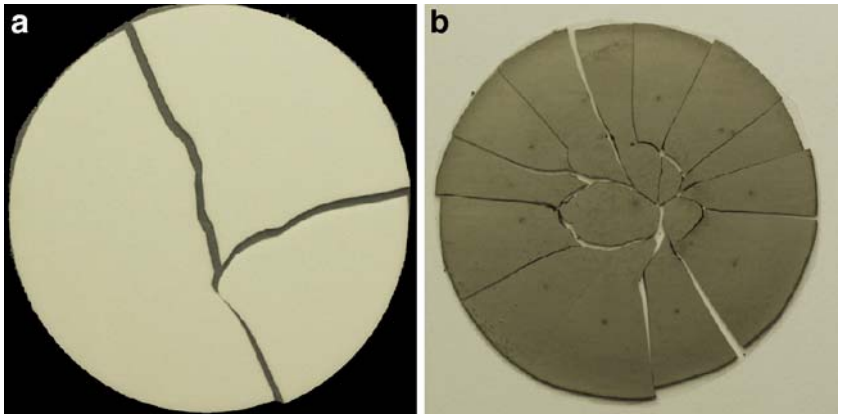

Fig. 8 Post ring-on-ring test photographs of Al_2O_3 (**a**) and SCF (**b**) showing low-strength and high-strength failure modes, respectively

and were tested in triplicate. The results are depicted in Figs. 7 and 8.

The elastic modulus of Al_2O_3 decreases from ~260 to ~210 GPa when the sample is heated from room temperature to 1,073 K, and that of SCF from ~100 to ~70 GPa. The tensile stress and ductility of Al_2O_3 increases with increasing temperature under the current conditions, and the stress–strain relation remains linear. It is, however, noted that alumina breaks in a low strength mode, induced by single defects (see Fig. 8). We also observe an increasing tensile strength and ductility with increasing temperature for SCF. However, in this case the breaking mode is of the high-strength type, indicating a very homogeneous material. The stress–strain relation becomes clearly curved at higher values. This is an indication for creep in this material that induces undesirable ductility. The resulting creep has also been studied by Majkic et al. for SCF [5, 34, 35].

Conclusions

Structural, chemical, mechanical, and transport properties of SCF and BSCF have been presented and discussed in conjunction with the findings of other authors. The main outcome of the present study on membrane materials for air separation membranes is that, from a point of view of required fluxes, both SCF and BSCF satisfy the minimum demand for economic viability, 10 ml/cm^2·min. Both compositions hold the promise of even larger fluxes under higher, industrial, driving forces. This leaves ample room for improvement in chemical and mechanical stability which will likely lead to a slight reduction in flux. Stabilizing additives to inhibit kinetic demixing and reduction phenomena, as well as for reducing creep and increasing strength, will be part of our research in the near future. The dual-phase concept and doping with tin- or zirconium-based oxides are seen as viable options to achieve "industrial grade" membranes. From the point of view of operational integrity, BSCF is preferred because, in the operational window of temperature and pressure, no phase transition to the vacancy-ordered brownmillerite structure is observed. However, the long-term stable performance remains to be confirmed.

Acknowledgements Financial support for Steven McIntosh was provided by the EU Marie Curie Intra-European Fellowship "OXYMEM." Further financial support was provided by the Dutch Ministry of Economic Affairs through the Energiebesparing Door Innovatie (EDI) program administered by Senter-Novem under contract number EDI03201.

References

1. Teraoka Y, Zhang HM, Furukawa S, Yamazoe N (1985) Chem Lett 1743
2. Qiu L, Lee TH, Liu M, Yang YL, Jacobson AJ (1995) Solid State Ion 76:321
3. Lee TH, Yang YL, Jacobson AJ, Abeles B, Milner S (1997) Solid State Ion 100:87
4. Li Y, Maxey ER, Richardson JW (2005) J Am Ceram Soc 88:1244
5. Majkic G, Wheeler L, Salama K (2000) Acta Mater 48:1907
6. McIntosh S, Vente JF, Haije WG, Blank DHA, Bouwmeester HJM (2006) Solid State Ion 177:283
7. Liu LM, Lee TH, Qiu L, Yang YL, Jacobson AJ (1996) Mater Res Bull 31:29
8. Prado F, Grunbaum N, Caneiro A, Manthiram A (2004) Solid State Ion 167:147
9. Grunbaum N, Mogni L, Prado F, Caneiro A (2004) J Solid State Chem 177:2350
10. Fan CG, Deng ZQ, Zuo YB, Liu W, Chen CS (2004) Solid State Ion 166:339
11. Tan L, Yang L, Gu X, Jin W, Zhang L, Xu N (2005) AIChE J 50:701
12. Tan L, Yang L, Gu X, Jin W, Zhang L, Xu N (2004) J Membr Sci 230:21
13. Shao Z, Yang W, Cong Y, Dong H, Tong J, Xiong G (2000) J Membr Sci 172:177
14. Kharton VV, Shaulo AL, Viskup AP, Avdeev M, Yaremchenko AA, Patrakeev MV, Kurbakov AI, Naumovich AN, Marques FMB (2002) Solid State Ion 150:229
15. Ishihara T, Tsuruta Y, Chunying Y, Tokada T, Nishiguchi H, Takita Y (2003) J Electrochem Soc 150:E17
16. Kharton VV, Yaremchenko AA, Shaulo AL, Patrakeev MV, Naumovich EN, Logvinovich DI, Frade JR, Marques FMB (2004) J Solid State Chem 177:26
17. Bredesen R, Sogge J (1996) In: Seminar on the ecological applications of innovative membrane technology in the chemical industry Chem/Sem. 21/R.12 Cetraro, Calabria

18. Viitanen MM, van Welzenis RG, Brongersma HH, van Berkel FPF (2002) Solid State Ion 150:223
19. Vente JF, Haije WG, IJpelaan R, Rusting FT (2006) J Membr Sci doi:10.1016/j.memsci.2005.10.044
20. Kruidhof H, Bouwmeester HJM, van Doorn RHE, Burggraaf AJ (1993) Solid State Ion 63–65:816
21. Vente JF, Haije WG, Rak ZS (2006) J Membr Sci 276:178
22. Wiik K, Aasland S, Hansen HL, Tangen IL, Ødegård R (2002) Solid State Ion 152–153:675
23. Zhang K, Yang YL, Ponnusamy D, Jacobson AJ, Salama K (1999) J Mater Sci 34:1367
24. Wang H, Tablet C, Feldhoff A, Caro J (2005) J Membr Sci 262:20
25. Kharton VV, Marques FMB (2002) Curr Opin Solid State Mater Sci 6:261
26. Yi J, Feng SJ, Zuo YB, Liu W, Chen C (2005) Chem Mater 17:5856
27. Tong J, Yang W, Zhu B, Cai R (2002) J Membr Sci 203:175
28. McIntosh S, Vente JF, Haije WG, Blank DHA, Bouwmeester HJM (2006) Chem Mater 18:2187
29. van Doorn RHE, Bouwmeester HJM, Burggraaf AJ (1998) Solid State Ion 111:263
30. van Veen AC, Rebeilleau M, Farruseng D, Mirodatos C (2003) Chem Commun 32
31. Wang H, Cong Y, Yang W (2002) Chin Sci Bull 47:534
32. McIntosh S, Vente JF, Haije WG, Blank DHA, Bouwmeester HJM (2006) Solid State Ion (in press)
33. Lide DR (1997) Handbook of chemistry and physics, 78th edn. CRC Press, Boca Raton
34. Majkic G, Wheeler L, Salama K (2000) Mater Res Soc Symp Proc 575:349
35. Majkic G, Mironova M, Salama K (2001) Phil Mag A 81:2675